An Overview of the MATISSE Instrument — Science, Concept and Current Status

Bruno Lopez[1]
Stéphane Lagarde[1]
Walter Jaffe[2]
Romain Petrov[1]
Markus Schöller[3]
Pierre Antonelli[1]
Udo Beckmann[4]
Philippe Berio[1]
Felix Bettonvil[5]
Andreas Glindemann[3]
Juan-Carlos Gonzalez[3]
Uwe Graser[6]
Karl-Heinz Hofmann[4]
Florentin Millour[1]
Sylvie Robbe-Dubois[1]
Lars Venema[5]
Sebastian Wolf[7]
Thomas Henning[6]
Thierry Lanz[1]
Gerd Weigelt[4]
Tibor Agocs[5]
Christophe Bailet[1]
Yves Bresson[1]
Paul Bristow[3]
Michel Dugué[1]
Matthias Heininger[4]
Gabby Kroes[5]
Werner Laun[6]
Michael Lehmitz[6]
Udo Neumann[6]
Jean-Charles Augereau[8]
Gerardo Avila[3]
Jan Behrend[4]
Gerard van Belle[9]
Jean-Philippe Berger[3]
Roy van Boekel[6]
Serge Bonhomme[1]
Pierre Bourget[3]
Roland Brast[3]
Olivier Chesneau[1†]
Jean-Michel Clausse[1]
Claus Connot[4]
Ralf Conzelmann[3]
Pierre Cruzalèbes[1]
Gergely Csepany[10]
William Danchi[11]
Marco Delbo[1]
Françoise Delplancke[3]
Carsten Dominik[12]
Albert van Duin[5]
Eddy Elswijk[5]
Yan Fantei[1]
Gerd Finger[3]
Armin Gabasch[3]
Jean Gay[1]
Paul Girard[1]
Vincent Girault[1]
Philippe Gitton[3]
Annelie Glazenborg[13]

Frédéric Gonté[3]
Florence Guitton[1]
Serge Guniat[3]
Menno De Haan[5]
Pierre Haguenauer[3]
Hiddo Hanenburg[5]
Michiel Hogerheijde[2]
Rik ter Horst[5]
Josef Hron[14]
Yves Hugues[1]
Christian Hummel[3]
Jan Idserda[5]
Derek Ives[3]
Gerd Jakob[3]
Attila Jasko[9]
Paul Jolley[3]
Sandor Kiraly[9]
Rainer Köhler[6]
Jan Kragt[4]
Tim Kroener[6]
Sjouke Kuindersma[5]
Lucas Labadie[15]
Christoph Leinert[6]
Rudolf Le Poole[2]
Jean-Louis Lizon[3]
Christian Lucuix[3]
Aurélie Marcotto[1]
Frantz Martinache[1]
Grégoire Martinot-Lagarde[1]
Richard Mathar[6]
Alexis Matter[8]
Nicolas Mauclert[1]
Leander Mehrgan[3]
Anthony Meilland[1]
Klaus Meisenheimer[6]
Jeffrey Meisner[2]
Marcus Mellein[6]
Serge Menardi[3]
Jean-Luc Menut[1]
Antoine Merand[3]
Sébastien Morel[3]
Lazlo Mosoni[10]
Ramon Navarro[5]
Edmund Nussbaum[4]
Sébastien Ottogalli[1]
Ralf Palsa[3]
Johana Panduro[6]
Eric Pantin[16]
Thierry Parra[1]
Isabelle Percheron[3]
Thanh Phan Duc[3]
Jörg-Uwe Pott[6]
Eszter Pozna[3]
Frank Przygodda[17]
Yves Rabbia[1]
Andrea Richichi[18]
Florence Rigal[5]
Ronald Roelfsema[5]
Gero Rupprecht[3]

Dieter Schertl[4]
Christian Schmidt[3]
Nicolas Schuhler[3]
Menno Schuil[5]
Alain Spang[1]
Jörg Stegmeier[3]
Lamine Thiam[1]
Niels Tromp[5]
Farrokh Vakili[1]
Martin Vannier[1]
Karl Wagner[6]
Julien Woillez[3]

[1] Laboratoire Lagrange, UMR7293, Université de Nice Sophia-Antipolis, CNRS, Observatoire de la Côte d'Azur, Nice, France
[2] Leiden Observatory, Leiden University, the Netherlands
[3] ESO
[4] Max-Planck Institute for Radio Astronomy, Bonn, Germany
[5] NOVA ASTRON, Dwingeloo, the Netherlands
[6] Max-Planck Institute for Astronomy, Heidelberg, Germany
[7] Institute of Theoretical Physics and Astrophysics, Kiel University, Germany
[8] Université de Grenoble Alpes, CNRS, IPAG, Grenoble, France
[9] Lowell Observatory, Flagstaff, USA
[10] MTA Research Centre for Astronomy and Earth Sciences, Konkoly Thege Miklos Astronomical Institute, Budapest, Hungary
[11] NASA/Goddard Space Flight Center, Greenbelt, USA
[12] Sterrenkundig Instituut "Anton Pannekoek", University of Amsterdam, the Netherlands
[13] Kernfysisch Versneller Institute, Groningen, the Netherlands
[14] Institut für Astrophysik, University of Vienna, Austria
[15] I. Physics Institute, University of Cologne, Germany
[16] Laboratoire AIM, CEA/DSM–CNRS–Université Paris Diderot, IRFU/Service d'Astrophysique, CEA-Saclay, Gif-sur-Yvette, France
[17] Deutsche Thomson OHG, Villingen-Schwenningen, Germany
[18] National Astronomical Research Institute of Thailand, Chiang Mai, Thailand

MATISSE, a second generation Very Large Telescope Interferometer (VLTI)

instrument, is a combined imager and spectrograph for interferometry in the 3–5 μm region (*L*- and *M*-bands) and the 8–13 μm window (*N*-band). MATISSE builds on the experience gained with the VLTI's first generation instruments. It employs multi-axial beam combination while also providing wavelength differential visibility and phase, and closure-phase aperture-synthesis imaging at a range of spectral resolutions. MATISSE is designed for a broad range of science goals, and its potential for studies of the discs around young stars and active galactic nuclei are highlighted. The instrument concept and operating modes are described; construction is in progress towards installation at the VLTI in 2016.

The Multi ApertTure mid-Infrared Spectro-Scopic Experiment (MATISSE) is the mid-infrared spectrograph and imager under construction for the VLTI. This second generation interferometric instrument will significantly contribute to several fundamental research topics in astrophysics, focussing, for instance, on the inner regions of discs around young stars where planets form and evolve, the surface structure and mass loss of stars at different evolutionary stages and the environment of black holes in active galactic nuclei (AGN).

MATISSE offers unique interferometric capabilities. The first is the opening of the *L*- and *M*-bands (respectively 3.0–4.0 and 4.6–5.0 μm) to long-baseline infrared interferometry. The angular resolution in the *L*-band will be about 3 milliarcseconds (mas) and various spectral resolutions between $R \sim 30$ and $R \sim 5000$ will be available. The second unique capability will be mid-infrared imaging — closure-phase aperture-synthesis imaging — performed with up to four Unit Telescopes (UTs) or Auxiliary Telescopes (ATs).

The MATISSE spectral bands will link the near-infrared spectral domain, for which several interferometric instruments have been developed, with the millimetre domain, where the Atacama Large Millimeter/Submillimeter Array (ALMA) provides a similar angular resolution. MATISSE can be seen as a successor to MIDI (the MID-infrared Interferometric instrument)

because it will reconstruct images in the mid-infrared. The extension of MATISSE down to the infrared *L*-band makes it also an extension of AMBER (the Astronomical Multi-BEam CombineR) and of the second generation instrument GRAVITY (Eisenhauer et al., 2011). MATISSE will also be complementary to METIS (the Mid-infrared E-ELT Imager and Spectrograph for the European Extremely Large Telescope): while MATISSE will provide an angular resolution higher by a factor ~ 4–5, METIS will yield a higher sensitivity, higher spectral resolution and a broader wavelength coverage.

We present some of the main science objectives that have driven the instrument design. We introduce the physical concept behind MATISSE, including a description of the signal on the detectors and an evaluation of the expected performance, and discuss the project status. The operations concept will be detailed in a future article, which will illustrate the observing templates that operate the instrument, the data reduction and image reconstruction software.

Scientific motivation

From the very beginning of the project, MATISSE was planned as an interferometric imager for a broad range of astrophysical targets. To achieve this goal, stringent requirements for the instrument were derived from the most challenging science cases (Lopez et al., 2013): protoplanetary discs around progenitors to Solar-type stars (T-Tauri stars) and the dusty tori around AGN. The expected and achieved instrument characteristics will also open up other fields: the study of the birth of massive stars; the structure, dynamics and chemistry of evolved stars; the early evolution of Solar System minor bodies; exo-zodiacal dust discs of stars; properties of hot Jupiters; and the study of the immediate vicinity of the Galactic Centre (Wolf et al., 2007). In the following, we present an overview of the key astrophysical questions for which significant progress can be expected from observations with MATISSE.

Circumstellar discs
In the specific case of circumstellar discs, MIDI and AMBER allowed observers, for

the first time, to investigate the potential planet-forming regions around young stars in nearby star-forming regions. The large-scale characteristics of these discs on scales of about 100 astronomical units (au) could be compared to the structure of the inner, au-scale regions (e.g., Leinert et al. 2004; Schegerer et al., 2009; Menu et al., 2014). Differences found in the grain size and crystallinity for the dust phase provided valuable insights into the physics determining the disc mineralogy (van Boekel et al., 2004), while the temporal variability of the re-emission brightness on scales of a few au sheds light on processes in young eruptive stars (Mosoni et al., 2013). In the near-infrared, AMBER was able to resolve the sub-au-scale gas and dust regions of accretion discs and the launching areas of winds in the continuum and emission lines (e.g., Br γ). Furthermore, the high spectral resolution offered by AMBER enabled the study of the kinematic properties of inner discs and disc wind regions (e.g., Weigelt et al., 2011). Such studies are important to improve our understanding of the fundamental accretion–ejection process.

MATISSE will allow us to continue from there, but with even more ambitious goals. This enthusiasm is justified on account of the following examples of the discovery potential of the instrument:
1. Direct detection of asymmetric disc structures, which can be used as tracers for the mechanisms of planet formation.
2. The extension to the *L*- and *M*-bands will allow the different spatial regions of the targeted objects, as well as different physical processes, to be investigated. While the *N*-band (7.5–14.5 μm) observations are dominated by the thermal emission of warm and cool dust, the *L/M*-band flux is expected to consist of both emission and scattering of short-wavelength radiation.
3. MATISSE will offer various spectral resolutions in the range of ~ 30 to ~ 5000, providing the means to study spectral features of amorphous and crystalline dust and polycyclic aromatic hydrocarbons (PAHs), as well as the distribution and kinematics of the gas.
4. Repeated observations will allow investigation of the temporal changes suggested from planet formation and planet–disc interaction scenarios.

Model ATs UTs Illustration
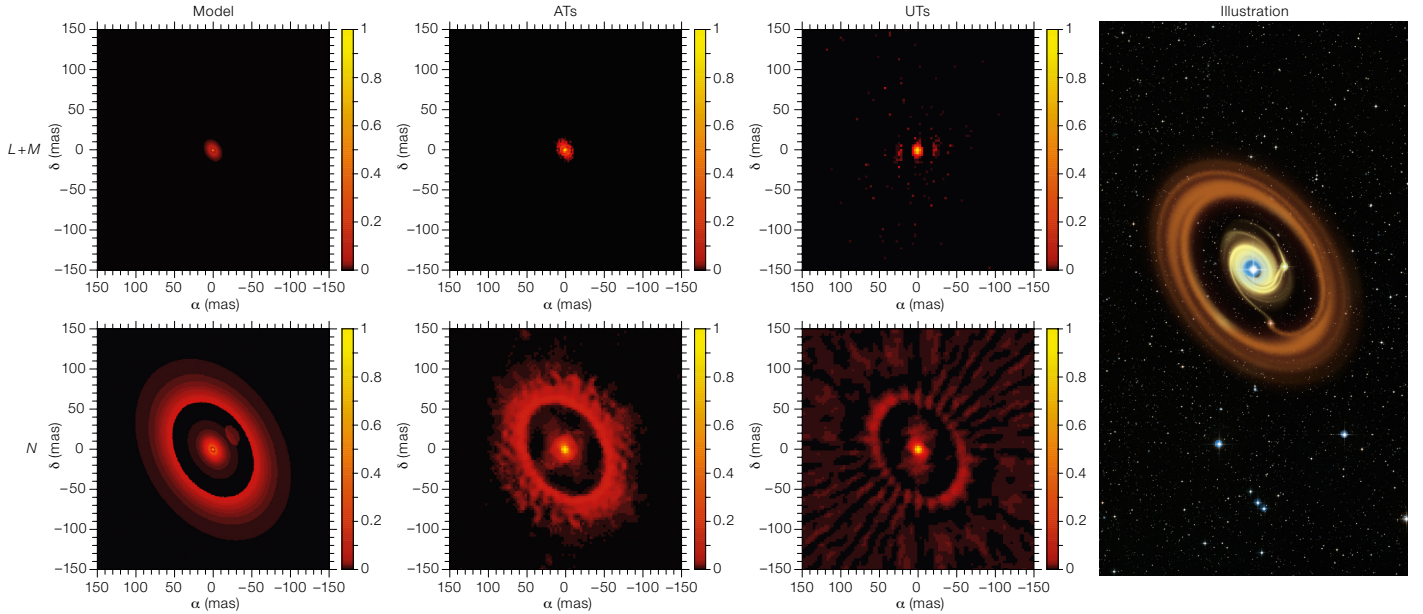
Figure 1. Illustration of the imaging capabilities of MATISSE in *L*-, *M*- and *N*-bands. A realistic scene representing the appearance of the young stellar object HD 100546 and its disc was simulated (left-most column), fed into a MATISSE instrument simulator assuming three nights (for the ATs, second column) or one night (for the UTs, third column) of data collection. The reconstructed images were made using the MIRA software (Thiébaut & Giovannelli, 2010) and are shown in the second and third columns. The rightmost image, the genesis of the model, is based on Crida et al. (2008) and Crida (private communication).

Feature	Wavelength (µm)
L- and *M*-bands (~ 2.8–5.0 µm)	
H_2O (ice)	3.14
H_2O (gas)	2.8–4.0
H lines (Br-α, Pf-β)	4.05, 4.65
PAHs	3.3, 3.4
Nano-diamonds	3.52
CO fundamental transitions	4.6–4.78
CO (ice)	4.6–4.7
N-band (~ 8.0–13.0 µm)	
Amorphous silicates	9.8
Crystalline silicates (olivines and pyroxenes)	9.7, 10.6, 11.3, 11.6
PAHs	8.6, 11.4, 12.2, 12.8
Fine structure lines (e.g., [S IV], [Ne III], [Ne II])	10.5, 10.9, 12.8

Table 1. Selected spectral signatures accessible with MATISSE.

In combination with other high angular resolution instruments/observatories operating at complementary wavelength ranges (e.g., GRAVITY and ALMA), MATISSE will provide the means to study the planet-forming region in detail (see Figure 1). Specific key topics and questions that MATISSE can tackle include: the complexity of disc structures in the planet-forming zone of circumstellar discs at various stages of their evolution; the reasons for inner-disc clearing in transitional discs; constraints on properties, growth, and sedimentation of dust grains; tracers for giant protoplanets; the nature of outbursting young stellar objects; dust production as an outcome of planetesimal collisions and evaporation of exo-comets; and the launching region of winds and jets and the disc–outflow connection. Important spectral features of the gas and dust phase in these objects that will be accessible to MATISSE are listed in Table 1.

Active galactic nuclei

The other major observational topic for MATISSE concerns the study of AGN. The wavelength and baseline configurations provided by the VLTI allow observers to investigate the gas emission and dust emission in the temperature range 300–1500 K in the 0.1–5-parsec core region of the nearest AGNs. Astrophysical problems that can be addressed with observations in the mid-infrared spectral domain concern the morphology, chemistry and physical state of the circumnuclear dusty structures. Important questions that MATISSE will be able to advance, are, for example: the relative distribution of the warm and the hot dust and the origin of this dust; the mechanism that supports the thickness and determines the inner edge of the dusty torus; the effect of the torus on the energy balance of the accreting material and the AGN as a whole; the origin of

the Type I/Type II dichotomy — as an inclination effect or fundamental morphological differences; and the relation between the dusty regions and the inner ionised broad line region (BLR).

The results achieved within studies of individual nearby bright AGNs with MIDI, AMBER and the Keck interferometer (Jaffe et al., 2004; Kishimoto et al., 2011; Meisenheimer et al., 2007; Petrov et al., 2012; Weigelt et al., 2012; Tristram et al. 2014; Lopez-Gonzaga et al., 2014) and the Large Programme survey of 25 Seyfert galaxies with MIDI (Burtscher & Tristram, 2013) have shown that warm (~ 300–1500 K) nuclear dust discs do indeed exist. However, in the *N*-band they appear smaller than expected (~ 1 pc), sometimes misaligned relative to the jets, and show indications of clumpiness. The spectrum of the silicate absorption does not resemble that in star-forming

regions. These results are interpreted as showing that the discs are comprised of dense clumps, optically thick even in the mid-infrared. Additional puzzling observations include the radio galaxy Centaurus A, which features a complicated mixture of thermal and synchrotron radiation and the quasar 3C273 (Petrov et al., 2012) with a BLR that extends beyond the inner edge of its dust torus.

MATISSE will allow us, for the first time, to reconstruct infrared aperture-synthesis images of the nearest AGN — NGC 1068, Circinus, and Centaurus A. Their mid-infrared dust emission in the circum-nuclear region was too complex for MIDI to disentangle and true mapping with closure phases is needed. MATISSE will allow the relative astrometry of features in these AGN to be probed over its broad wavelength range (3–13 μm).

However, to make full use of the potential of MATISSE and thus to fully achieve the above goals, improvements in the VLTI infrastructure are mandatory. In particular, these concern the decrease of the vibration level of the UTs, adaptive optics on the ATs, and, most important, the availability of a second generation fringe tracker (2GFT) for MATISSE. A 2GFT will improve the sensitivity, accuracy and spectroscopic capability of MATISSE and will thus have a direct impact on the scientific potential of the instrument, in the following ways:

– The sensitivity achievable with a 2GFT is required for the study of AGNs and the discs around young stars. For example, with a 2GFT, longer baselines can be used to establish the connections between the high surface brightness inner discs and the asymmetric larger components.
– Higher accuracy is important for closure-phase imaging in the *L*-, *M*- and *N*-bands, which provides constraints on the radial and vertical temperature gradient and opacity structure in discs of young stars.
– Medium and high spectral resolution interferometry will become feasible.

MATISSE concept

MATISSE uses an all-in-one multi-axial beam combination scheme. We concluded that this type of combination is the most suitable for an interferometric instrument with more than two apertures and operating in the mid-infrared. Initially, based on the efficiency of the two-telescope MIDI recombination scheme, a pairwise co-axial concept was considered. The advantage of this scheme is the simultaneous delivery of two interferometric signals per baseline, phase shifted by π. The correlated flux is then obtained by subtracting the two signals. In this way, the thermal background level and its associated temporal fluctuations are directly eliminated, but not the related thermal photon noise. However, in spite of good expected efficiency in terms of signal-to-noise ratio (SNR), this scheme displays a number of issues when extended from two to four telescopes: a possible weakness in the stability of the closure-phase measurements and a high instrumental complexity due to numerous opto-mechanical elements required in the cold environment. These issues led us to consider multi-axial global combination as the more robust and simpler scheme.

The multi-axial global beam combination scheme (see Figure 2) means that the four beams are combined simultaneously on the detector. The interferometric fringe pattern and the four individual photometric signals receive respectively 67 % and 33 % of the incoming flux. MATISSE will observe in three bands simultaneously: *L*, *M* and *N*. The signals are spectrally dispersed using grisms: spectral resolutions of 30 and 220 are provided in the *N*-band and four resolutions in the *L*- and *M*-bands of 30, 500, 1000 and 3500–5000. The spatial extent of the interferometric pattern is larger than the photometric signals in order to optimise the sampling of the six different spatial fringe periods. The beams are combined by the camera optics. At this plane, the beam configuration is non-redundant in order to produce different spatial fringe periods, and thus to avoid crosstalk between the fringe peaks in Fourier space. The separation B_{ij} between beams *i* and *j* in the output pupil is respectively equal to 3*D*, 9*D* and 6*D*, where *D* is the beam diameter.
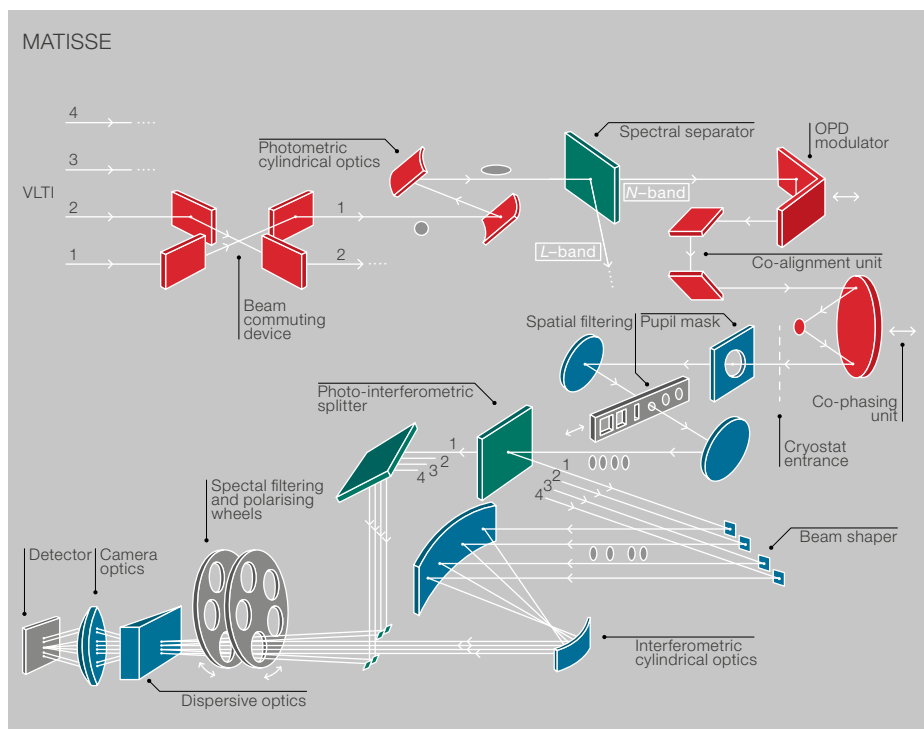

Figure 2. The schematic layout of the MATISSE instrument concept is shown. The red parts represent optical elements located on the warm optics table at ambient temperature. The blue parts represent optical elements of the cold optics bench located in the cryostats. Only one COB with its elements and detector is shown.

Since the thermal background at the longest wavelengths is variable, and much exceeds the target coherent flux, it is important to limit the cross-talk between the low frequency peak and the high frequency fringe peaks to a level below the thermal background photon noise limit. Two methods are used in MATISSE to ensure this result and estimate the coherent flux with high accuracy: spatial modulation, as in AMBER, and temporal modulation, as in MIDI, with both methods combined by varying the optical path difference (OPD) between the beams.

For each of the six baselines used and in each of the spectral channels, the observable quantities are the following:
1. photometry;
2. coherent flux of the source;
3. absolute visibility derived from the photometry and the coherent flux measurements;
4. wavelength-differential visibility (i.e., change of visibility with wavelength);
5. wavelength-differential phase; and
6. closure phase.

In order to measure the visibility, we need to extract the source photometry by separating the stellar flux from the sky background using sky chopping. The problem with chopping is that the observation of the sky and that of the target are not simultaneous. Therefore, thermal background fluctuations will be the most important contribution to the visibility error. Fortunately, chopping is unnecessary for measuring the coherent flux, the wavelength-differential and closure phases.

Operating modes

MATISSE has two standard operating modes. The HighSens mode does not provide photometry and all photons are collected in the interferometric fringe pattern beam. This maximises the sensitivity for the wavelength-differential and closure phases. In this mode it is possible to make photometric observations sequentially after the interferometric observations. In the SiPhot mode, two thirds of the flux goes into the interferometric channel and one third into the photometric channels. Chopping is used
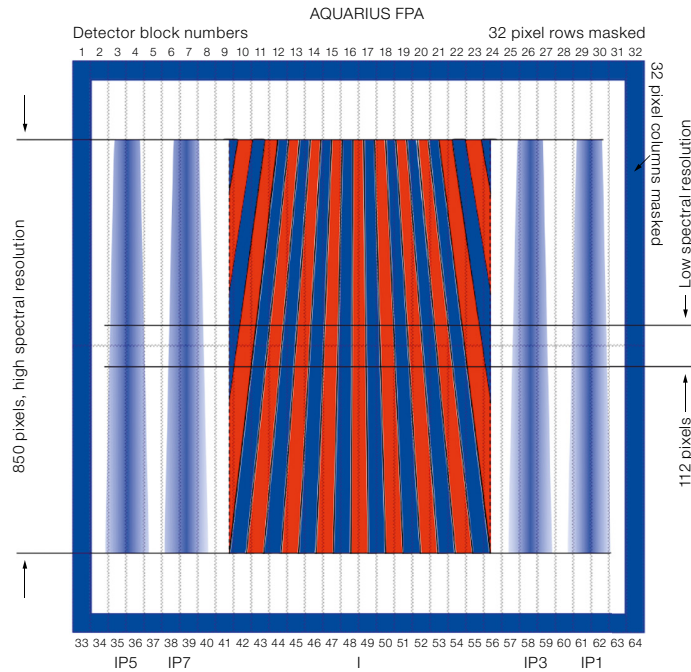
Figure 3. The layout of the interferometric pattern (central detector blocks, dispersion direction vertical) and the four photometric signals (outer detector blocks) on the AQUARIUS detector is shown for the SiPhot mode in N-band with medium spectral resolution dispersion.

to measure the average source photometry and extract the visibility from the coherent flux. These two modes can also be mixed, that is the HighSens mode in N-band and the SiPhot in L-band.

In the SiPhot mode, the detector simultaneously collects the light of up to five instrument outputs: four photometric signals in addition to the interferometric pattern (see Figure 3). During observations with four telescopes, the interferogram contains the combined dispersed fringe pattern of six baselines, but because the beam combination is non-redundant, the information on the fringes corresponding to six different spatial periods can directly be recovered. In the spatial direction, minimum sampling of the interferometric signal requires 4 pixels per period of the narrowest fringes (24 for the widest) at the short end of the spectral bands covered by the instrument. The sampling of the interferometric beam is 72 pixel per λ/D in the spatial direction and 3 pixels per λ/D in the spectral direction, corresponding to an anamorphic factor of 24.

In the spatial direction, the interferometric field is about 468 pixels wide (corresponding to a field of 4λ/D) and the photometric field is about 78 pixels. The size in the spectral direction depends on the spectral resolution and varies from 100 pixels for L- and M-bands at low spectral resolution (150 pixels for the N-band at low resolution) to the full detector for medium and high spectral resolution (indicated on Figure 3).

Performance

Tables 2 and 3 give the limiting fluxes and specifications for MATISSE. The values take into account all characteristics of the VLTI (e.g., optical transmission, adaptive optics performance, tip-tilt, focal laboratory) and a full calibration procedure (Lagarde et al., 2012).

The expected ultimate performance requires some evolution of the VLTI infrastructure: external fringe tracking, collecting data such as OPD and tip-tilt residu-

	L-band sensitivity	N-band sensitivity
AT	Spec = 6.5 Jy (L = 4.1), Goal = 1.25 Jy	Spec = 45 Jy (N = −0.25), Goal = 10 Jy
UT	Spec = 0.65 Jy (L = 6.6), Goal = 0.12 5Jy	Spec = 3 Jy (N = 2.7), Goal = 0.75 Jy

Table 2. L- and N-band limiting fluxes.

		L-band	N-band
Visibility	AT	≤ 7.5 % (Goal: 2.5 %)	≤ 30 % (Goal: 10 %)
	UT	≤ 7.5 % (Goal: 2.5 %)	≤ 7.5 % (Goal: 2.5 %)
Closure phase	AT	≤ 80 mrad	≤ 80 mrad
	UT	≤ 40 mrad	≤ 40 mrad
Differential visibility	AT	≤ 3 % (Goal: 1 %)	≤ 30 % (Goal: 10 %)
	UT	≤ 1.5 % (Goal: 0.5 %)	≤ 5 % (Goal: 2 %)
Differential phase	AT	≤ 60 mrad	≤ 60 mrad

Table 3. L- and N-band specifications (and goals) for a 20 Jy unresolved source observed at low spectral resolution.
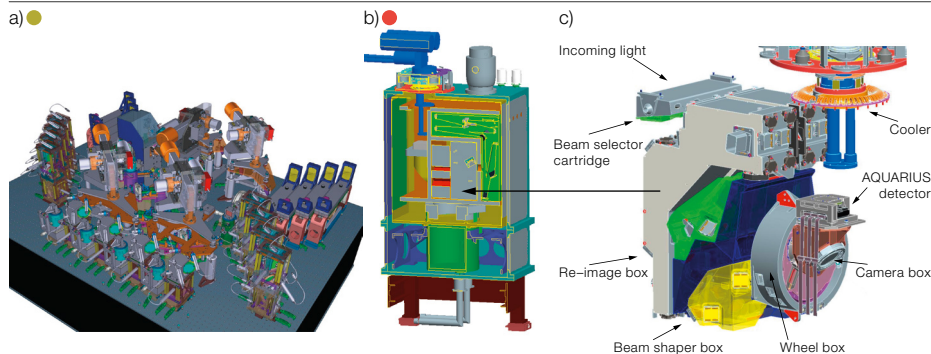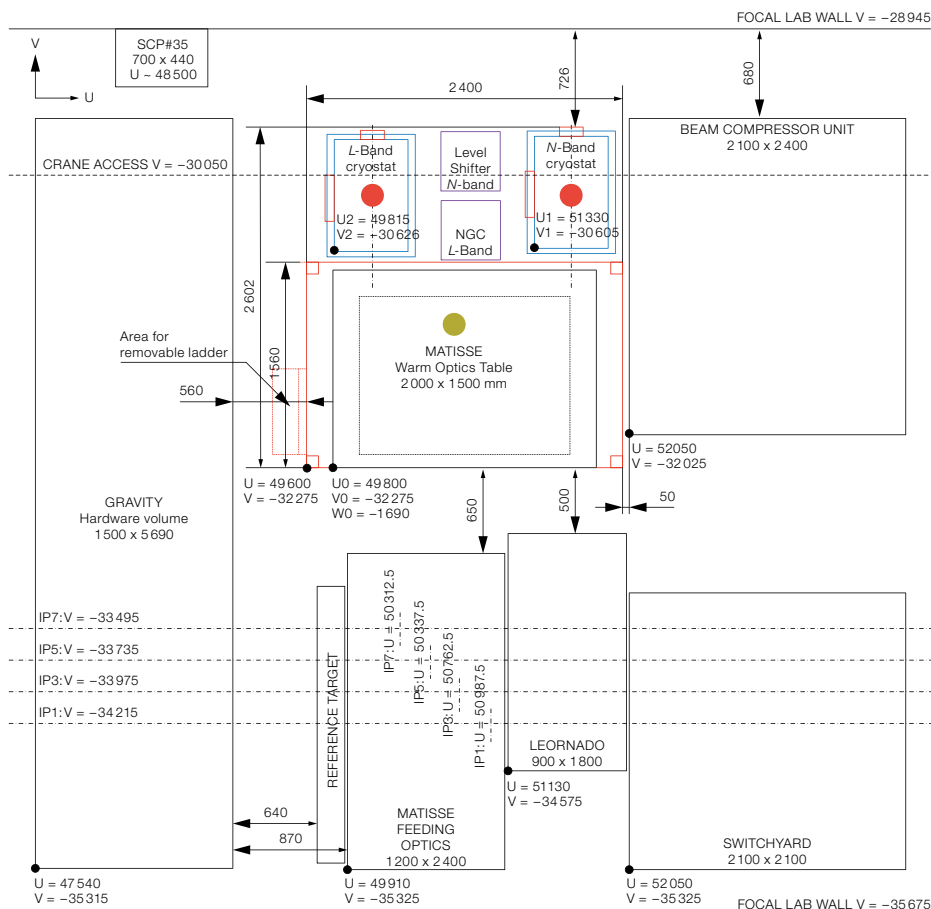

a) ●   b) ●   c)

Figure 4. The future location of MATISSE in the VLTI laboratory is sketched. The warm optics table and the two cryostats are viewed from above. This location is currently used by MIDI. Sub-figure (a) shows the MATISSE warm optics bench with its optical components; (b) one of the two MATISSE cryostats, which holds the cold optics bench and the detector; and (c) shows one of the MATISSE cold optics benches.

als, and lateral pupil motion monitoring or even active correction.

Instrument design

MATISSE is composed of the Warm OPtics (WOP) and two Cold Optics Benches (COB). There are two mid-infrared detectors, each housed, with a COB, in its own cryostat; see Figure 2 where only a single COB is sketched. The locations of the different parts of the instrument inside the VLTI laboratory are illustrated in Figure 4.

The WOP rests on a 2 by 1.5 metre optical table and receives four beams — designated IP7/5/3/1 — through the feeding optics, coming from either the UTs or ATs. These four beams enter first into the beam commuting devices, which allow the commutation of beams IP7 and IP5 and beams IP3 and IP1. The beams are then individually anamorphosed with a ratio of 1:4 by the cylindrical optics. The beams are spectrally separated with individual dichroics in order to form the L- and M-band and the N-band beams. Before entering into the cryostats, each beam passes through two modules. The first one is a periscope that is used for the co-alignment of image and pupil. The second module is a delay line that delivers the pupil plane at the correct position into the COB and equalises the optical path differences between the beams and the differential optical path between the L- and M- and the N-bands.

The WOP also contains the OPD modulation function, which is part of the spectral separator. In addition, the WOP accommodates two internal optical sources in a tower, one visible light source for alignment purposes (a fibred laser diode) and one infrared source for calibration purposes (a ceramic with thermal insulation housing). These internal optical sources deliver four identical beams and are injected into the instrument through the SOurce Selector module (SOS).

The cold optics benches consist of several modules. The beam selector cartridge holds four shutters. The re-imager box supports the cold stop in the pupil plane, curved optics and the spatial filters in

the image plane with its pinhole and slit slider. The beam-shaper box contains the beam splitters with a slider, several folding mirrors, the anamorphic optics and the photometric re-injection mirrors. The wheel box includes the filter wheel, the polarising wheel and the dispersive wheel and the camera box carries the two camera lenses, a folding mirror and the detector mount (see Figure 2).

Light enters the entrance windows of the cryostats with an anamorphic factor of 4, passing the cold stops and the off-axis optics and spatial filtering module of the re-imager unit, until it reaches the beam splitter. The light is split into the interferometric channel and the photometric channels. The anamorphism of the interferometric channel is further increased by a factor of 6, to a total of 24 by the anamorphic optics. Finally, after passing the filter, polariser and dipersion wheels, the light will reach the detector via the camera (Figure 2).

MATISSE uses two different detectors. The MATISSE *L*- and *M*-band detector is a Teledyne HAWAII-2RG of 2048 × 2048 pixels, grouped in 32 blocks of 64 × 2048 pixels. The MATISSE *N*-band detector is a Raytheon AQUARIUS, which has a format of 1024 × 1024 pixels, grouped in 2 × 32 blocks of 32 × 512 pixels.

Genesis and future of the project

In 2002 the two-telescope VLTI instrument MIDI had first light. Already at that time, the idea of an upgrade to an interferometric imager was born. A first prototype was studied and built, leading to a first concept, called APreS-MIDI (Aperture SynthesiS with MIDI), which was presented at the ESO VLTI conference in 2005 (Richichi et al., 2008).

Following a recommendation by ESO, the MATISSE Consortium initiated a conceptual design study for a second generation VLTI instrument. The MATISSE Preliminary Design Review was held in December 2010 in Garching, and the Final Design Reviews occurred in September 2011 for cryogenics and optics and April 2012 for the whole instrument. Currently, we are building the instrument;
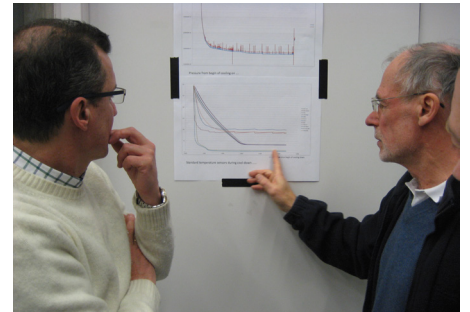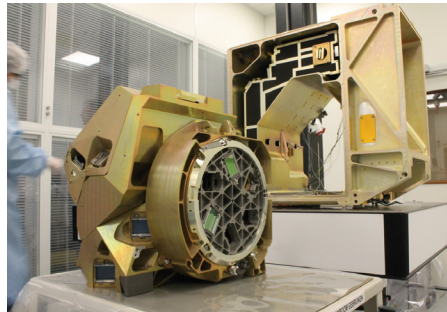

Figure 5. Some views from the laboratories: 5a: A view of some of the components of the cold optics bench, including the beam-shaper box presented in front of the COB backbone; 5b: A discussion concerning the cool-down procedure; 5c: Two of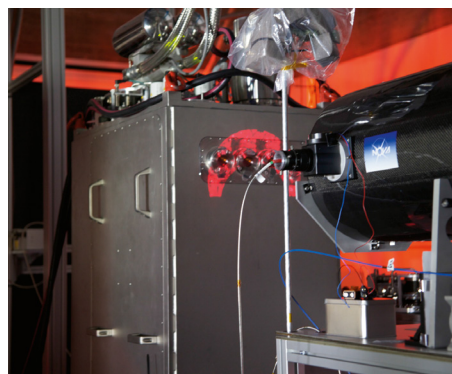 the three electronics cabinets; 5d: Both cryostats at MPIA; 5e: The *N*-band cryostat and cold optics delivered to Nice in July 2014 and now installed in front of the warm optics bench. This moment marks the beginning of the global integration of all the MATISSE subsystems.

preliminary acceptance in Europe is planned for November 2015 and the first light at Paranal is foreseen in 2016.

The project became possible thanks to the scientific research conducted in our laboratories and institutes in the field of interferometric concepts and observing methods and the experience acquired on AMBER and MIDI. The availability of several new key technological components, like large detectors, efficient cooling devices and state-of-the-art cryo-mechanisms have contributed to make MATISSE possible and enable a highly automated instrument. The numerous interactions between people and institutes from different countries as well as the engineering challenges have made our project a pleasant human adventure that has generated a lot of creativity.

As a general user instrument, the aim is that MATISSE observations should be conducted by many researchers from the international community. MATISSE will offer unique and fascinating observational capabilities: new spectral observing windows at the VLTI and closure-phase image reconstruction in the mid-infrared. The high-resolution observations of young circumstellar discs where planets form and evolve, of surface structures and mass-loss of stars in late evolutionary stages, and of the environments of black holes in AGN will contribute to

answering several fundamental astrophysical questions and will surely lead to unexpected discoveries. We hope that all future observers will benefit from use of MATISSE.

Status of the project

The different MATISSE subsystems are being integrated and tested at the NOVA-ASTRON Institute in Dwingeloo, the Max-Planck Institute for Astronomy in Heidelberg (MPIA), the Max-Planck Institute for Radio Astronomy in Bonn (MPIfR), the detector department of ESO Garching and the Observatory of the Côte d'Azur (OCA) in Nice.

Figure 5 shows some views of the different subsystems integrated in our laboratories. Figure 6 shows images from the first laboratory fringes obtained in spring 2014. It shows the first infrared illumination and fringes on the AQUARIUS detector. A mid-infrared laser beam was feeding three of the four MATISSE beams.

The different subsystems integrated and tested in the different institutes of the Consortium are presently being sent to OCA for global integration and testing of the instrument. Following delivery of part of the electronics and the instrument software from MPIA to OCA in April 2014, the N-band cold optics, its cryostat and the AQUARIUS detector are being delivered in the period July–September 2014. The L- and M-band COB with its cryostat, its HAWAII 2RG detector and its electronics, will be sent from MPIA to Nice in November 2014.

References

Burtscher, L. et al. 2013, A&A, 558, A149
Burtscher, L. & Tristram, K. R. W. 2013,
    The Messenger, 154, 62
Crida, A. et al. 2008, A&A, 483, 325
Eisenhauer, F. et al. 2011, The Messenger, 143, 16
Jaffe, W. et al. 2004, Nature, 429, 47
Kishimoto, M. et al. 2011, A&A, 536, 78
Lagarde, S. et al. 2012, SPIE, 8445-91
Lopez, B. et al. 2013, MATISSE Science Analysis
    Report, Issue 4
Lopez-Gonzaga, N. et al. 2014, A&A, 565, 71
Leinert, C. et al. 2004, A&A, 423, 537
Meisenheimer, K. et al. 2007, A&A, 471, 453
Menu, J. et al. 2014, A&A, 564, A93
Mosoni, L. et al. 2013, A&A, 552, A62
Petrov, R. G. et al. 2012, SPIE, 8445-0W
Richichi, A. et al. (eds.) 2008, *The Power of Optical/
    IR Interferometry: Recent Scientific Results and
    2nd Generation VLTI Instrumentation*, Proc. ESO
    Workshop, Springer
Schegerer, A. A. et al. 2009, A&A, 502, 367
Thiébaut, E. & Giovannelli, J. F. 2010, IEEE Signal
    Processing Magazine, 27, 97
Tristram, K. R. W. et al. 2014, A&A, 563, A82
van Boekel, R. et al. 2004, Nature, 432, 479
Weigelt, G. et al. 2011, A&A, 527, A103
Weigelt, G. et al. 2012, A&A, 541, L9
Wolf, S. et al. 2007, MATISSE Phase A Science
    Cases, Issue 1

Figure 6. Images from the observation of the first fringes in spring 2014 in the laboratory at MPIA are shown in 6a and 6b. The zoom on the computer screen during the first fringe event is shown in 6c. Only three input beams were used for this test. The spatial direction is horizontal and the spectral dispersion vertical. On the left and right of the screen the photometric channels can be seen (c.f. Figure 3).